

Effect of impurity ions on the charge separation and velocity shear at a plasma edge

M. Shoucri, E. Pohn,^{a)} P. Bertrand,^{b)} G. Knorr,^{c)} G. Kamelander,^{a)} G. Manfredi,^{b)} and A. Ghizzo^{b)}

Centre Canadien de Fusion Magnétique, Varennes, Québec, Canada J3X 1S1

(Received 15 December 1998; accepted 28 January 1999)

The problem of the formation of charge separation in a plasma in the presence of a steep density gradient, the self-consistent electric field and the associated $E \times B$ velocity, are studied using a two-dimensional (2D) gyro-kinetic Vlasov code for the ions, with electrons following an adiabatic law. The code shows the formation of a one-dimensional (1D) equilibrium charge at the plasma edge. It is also shown that the presence of a small fraction of impurity ions at the plasma edge can have a significant effect in increasing the effective charge separation and the associated electric field. The present results show that only a kinetic code can solve the problem of the equilibrium electric field in the presence of a density gradient, and point to the important role played by the ions' gyro-radius in establishing a charge separation at a plasma edge. © 1999 American Institute of Physics. [S1070-664X(99)02605-1]

The problem of the existence of an equilibrium charge separation in a plasma in the presence of a density gradient is of major importance in the edge plasma physics and reversed shear equilibria associated with tokamaks, as well as in many problems associated with plasma vacuum and plasma wall transitions. We present in this work results obtained using a two-dimensional (2D) gyro-kinetic code for the ions with electrons following an adiabatic law. Details on the code have been previously published.^{1,2} The code shows the formation of a 1D equilibrium charge at the plasma edge, which is stable to perturbations. It also shows that the presence of a small fraction of impurity ions at the plasma edge can have a significant effect in increasing the effective equilibrium charge separation at the plasma edge in the presence of a density gradient. Attention has long been pointed to the important role played by small fractions of impurity ions in the peripheral region of a tokamak plasma, both in the excitation of modes driven by the density gradient which control the energy transport in the plasma edge,^{3,4} and in the fact that a small quantity of impurity greatly enhances the radiation losses in the plasma.⁵ However, impurity ions, having different gyro-radii from those of the main plasma ions, have a significant effect in modifying the effective charge at a plasma edge, and the self-consistent electric field. The present work is a contribution to this problem.

The pertinent equations for the gyro-kinetic code have been previously reported.^{1,2} We consider a two-dimensional slab geometry, x being the periodic (poloidal) direction and y the nonperiodic (radial) direction. The magnetic field B is situated in the (x, z) plane and makes an angle θ with the x axis. So any 2D charge separation is located in the (x, y) plane, and z is the homogeneous toroidal direction. We assume that the motion perpendicular to the magnetic field is completely described by the $E \times B$ drift and the polarization drift. We include in the equations a correction which takes into account the finite Larmor radius effect for the ions. The

pertinent equation for the ion distribution function f_i is given by:^{1,6}

$$\frac{\partial f_i}{\partial t} + \nabla \cdot (v_{\perp} f_i) + v_{\parallel} \cos \theta \frac{\partial f_i}{\partial x} + \frac{e}{m_i} E_x^* \cos \theta \frac{\partial f_i}{\partial v_{\parallel}} = 0, \quad (1)$$

$$v_{\perp} = v_D + v_{pi}, \quad v_D = E^* \times B / B^2, \quad (2)$$

$$v_{pi} = \frac{m_i}{e B^2} \left[\frac{\partial E_{\perp}^*}{\partial t} + (v_D + v_{\parallel}) \cdot \nabla_{\perp} E_{\perp}^* \right]. \quad (3)$$

A similar equation holds for impurity ions with Ze substituted instead of the charge e and m_I instead of m_i . The star over a quantity is an abbreviation for an integral operator that takes into account the finiteness of the ion Larmor radius,^{2,6}

$$a^*(r) = \int G(r - r') a(r') dr', \quad (4)$$

where $G(r)$ is a Gaussian kernel. In Fourier space, this operation becomes a filtering operation, which is numerically easy to perform: each coefficient of the $e^{ik \cdot r}$ mode is multiplied by a factor $G_k = \exp(-k_{\perp}^2 \rho_{i,I}^2 / 2)$, where $\rho_{i,I}$ is the Larmor radius for ions and impurity ions ($\rho_{i,I} = v_{ti,I} / \omega_{ci,I}$). Since the system is finite in the y direction, we convolute the function in Eq. (4) by first mirroring the function at the right boundary in y and thus doubling the y interval. We then take the Fourier transform and multiply the coefficients by $\exp(-k_{\perp}^2 \rho_{i,I}^2 / 2)$, and then the function is Fourier transformed back.

The Poisson equation reads as follows:

$$\Delta \varphi = -4\pi e (n_i^* + n_I^* - n_e), \quad E = -\nabla \varphi, \quad (5)$$

and $n_{i,I} = \int f_{i,I} dv_{\parallel}$ and the star over $n_{i,I}$ indicates again the filtering operation defined in Eq. (4). The electron density n_e in Eq. (5) is calculated from an adiabatic law,

$$n_e = n(y) e^{e\varphi / T_e}. \quad (6)$$

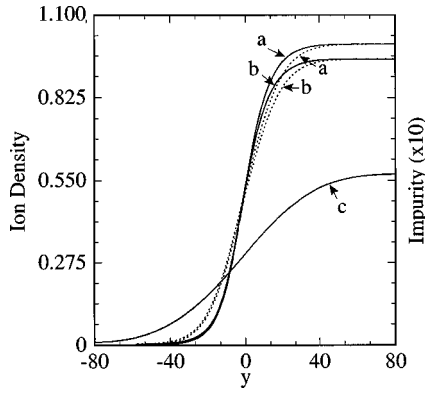


FIG. 1. Ion density profile n_i (full curve), and the corresponding profile n_i^* calculated from Eq. (4) (dotted curve) at the final equilibrium, calculated from the gyro-kinetic code, for: (a) no impurity ions; (b) 5% impurity ions with $m_i/m_e = 10$. Also shown is the density n_i^* of the impurity for [curve (c), vertical scale is magnified by a factor of 10].

We first start our calculation without impurity ions and take as initial ion density,

$$n_i = n(y) = 0.5(1 + \tanh(y/15)). \quad (7)$$

The initial distribution function for the ions is given by

$$f_i(x, y, v_{\parallel}) = \frac{n_i}{\sqrt{2\pi T_i}} e^{v_{\parallel}^2/2T_i(y)}. \quad (8)$$

The relevant physical parameters, in dimensionless form, are chosen as follows:

$$T_e/T_{io} = 1; \quad m_i/m_e = 1840; \quad \omega_{ci}/\omega_{pi} = 0.1,$$

and the ratio of the ion gyro-radius to the Debye length is given by

$$\rho_i/\lambda_{De} = \frac{v_{ti}/\omega_{ci}}{\lambda_{De}} = \frac{\sqrt{T_{io}/T_e}}{\omega_{ci}/\omega_{pi}} = 10. \quad (9)$$

Details of the numerical code have been previously presented.^{1,6} The boundary conditions on the distribution function are to set f_i equal to zero for $|v_{\parallel}| > V_{\max}$ in velocity space. In configuration space, periodicity is assumed in the x direction. In the nonperiodic y direction, the distribution function was forced to be equal to zero on one extra point outside the domain on the left, and to be identical to the last point on the right on one extra point outside the domain. The computational domain is $0 \leq x \leq 128$, $-80 \leq y \leq 80$, $-5 \leq v_{\parallel} \leq 5$. The number of grid points is $N_x N_y N_v = 64 \times 256 \times 128$. Time is normalized to ω_{pi}^{-1} , velocity to the acoustic velocity $C_s = \sqrt{T_e/m_i}$ and length to $C_s \omega_{pi}^{-1}$. Our simulation was performed with $\theta = 89^\circ$ and with a temperature profile

$$T_i(y) = T_{io}(0.2 + 0.4(1 + \tanh(y/10))), \quad (10)$$

with $T_{io} = T_e = 1$. We note that this temperature profile is for the parallel to be magnetic field velocity direction [see Eq. (8)]. The operation effected in Eq. (4) assumes a uniform temperature T_{io} in the direction perpendicular to the magnetic field. The potential is normalized to T_e/e . Any charge separation function of one space variable y is an equilibrium solution of Eq. (1),¹ since in this case $E_x = 0$. However, in

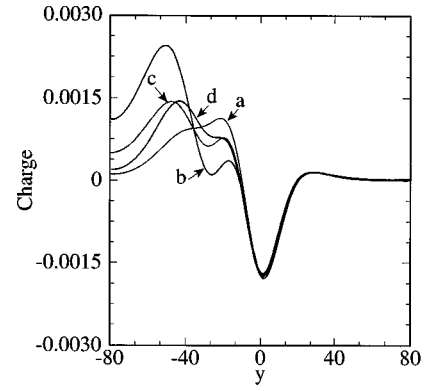


FIG. 2. Charge separation $n_i^* + n_i^* - n_e$: (a) no impurity ions $n_i^* = 0$; (b) with 5% impurity ions with $m_i/m_e = 10$; (c) with 2% impurity ions with $m_i/m_e = 10$; (d) with 5% impurity ions with $m_i/m_e = 5$.

view of the fact that E_y has to be calculated from Eqs. (5) and (6), one has to iterate a few hundred iterations between Eqs. (1) and Eqs. (5) and (6), starting from Eqs. (7) and (10), to reach the 1D self-consistent equilibrium. The initial profile $n_i = n(y)$ is relaxed to the profile shown in Fig. 1. This equilibrium is stable in the sense that if the system is perturbed by a perturbation $\sim \varepsilon \cos k_x x$, the perturbation damps, leaving the one-dimensional system in equilibrium. The corresponding electron density calculated from Eq. (6) is very close to the curve n_i^* in Fig. 1. Indeed, in Fig. 2(a) the charge $(n_i^* - n_e)$ presented at the final equilibrium is small. However, this small charge separation appearing in the tail of the density profile results in an important potential shown in Fig. 3(a), due to the large ratio ρ_i/λ_{De} . This can be also understood if Eq. (5) is normalized to the ion gyro-radius, instead of the Debye length. In this case, Eq. (5) is written

$$\nabla^2 \varphi = - \left(\frac{\rho_i}{\lambda_{De}} \right)^2 (n_i^* + n_i^* - n_e). \quad (11)$$

For $\rho_i/\lambda_D = 10$ as in the present calculation, any small charge separation appearing in Eq. (11) will be multiplied by a factor of 100. We have solved Eq. (11) applying the condition of zero potential at both boundaries, but this is not a

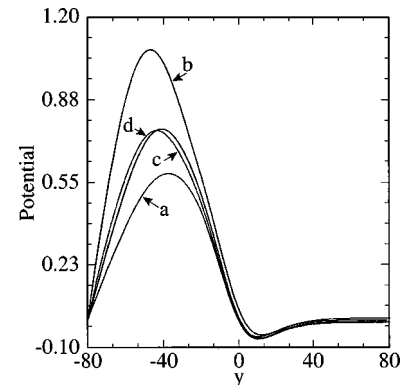


FIG. 3. Equilibrium potential calculated from the gyro-kinetic code: (a) no impurity ions; (b) with 5% impurity ions with $m_i/m_e = 10$; (c) with 2% impurity ions with $m_i/m_e = 10$; (d) with 5% impurity ions with $m_i/m_e = 5$.

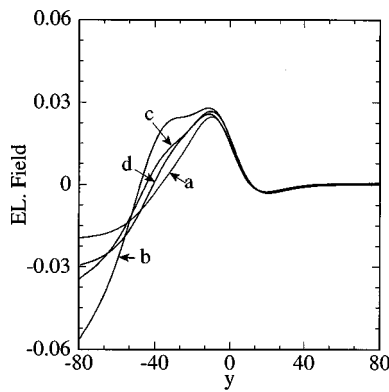


FIG. 4. Electric field profile E_y calculated with the gyro-kinetic code at the final equilibrium: (a) no impurity ions; (b) with 5% impurity ions with $m_i/m_e=10$; (c) with 2% impurity ions with $m_i/m_e=10$; (d) with 5% impurity ions with $m_i/m_e=5$.

restriction and φ or $\partial\varphi/\partial y$ can be arbitrarily fixed at the boundaries. Finally, the electric field $E_y = -\partial\varphi/\partial y$ at the final equilibrium is shown in Fig. 4(a).

We now add a small fraction of impurity ions with $n_i = 0.05n(y)$, and use $n_i = 0.95n(y)$ for the main ion species. We also assume $T_i = T_e$, and that the impurity ions are singly ionized ($Z=1$), and $m_i/m_e=10$. In this case the impurity gyro-radius is the order of 30, of the order of the scale length of the temperature variation in Eq. (10). However, results obtained for wider systems give essentially the same qualitative results. We use for the impurity ions another set of equations similar to Eqs. (1) and (8). Figure 1(c) shows the impurity density n_i^* , which gives a contribution in the tail of the profile (at the left boundary) as important as the main ion contribution (note the factor of 10 in the right vertical scale). Figure 2(b) shows the charge separation ($n_i^* + n_i^* - n_e$) obtained in this case, which shows a small difference toward the left boundary (where density is depleted) with the charge obtained when $n_i \neq 0$, due to the fact that the impurity has a larger gyro-radius than the main ion species. The impurity ions, having a larger gyro-radius, add a small contribution to the charge closer to the left boundary (even though they are only a small fraction), in a location where the main ions have only a very small contribution. However, this small difference translates into an important difference in the potential in Fig. 3(b) [see to the factor $(\rho_i/\lambda_{De})^2$ in Eq. (11)] and in the electric field at the edge in Fig. 4(b) [which is close to the double of the electric field when $n_i=0$ in Fig. 4(a)].

We note also in Fig. 4 that a small positive bump always appears in the profile of the electric field (transport barrier?), corresponding to the small negative potential well appearing in the potential profile in Fig. 3. The presence of this positive electric field bump is confirmed by results obtained in a 1D fully kinetic code. The electric field profile can, in reality, be much bigger. In the present simulation, we have used $m_i/m_e=10$. In practical experimental situations, this ratio can be much higher (krypton was used in the results presented in our Ref. 7), which will result in a larger gyroradius, and many impurities can be present which will result in a positive electric field wider than the bump we are presenting. For ions with charge number $Z \geq 2$, a random walk diffusion

can be caused by the fluttering of the gyro-radius as a result of successive recombination and ionization events. Neutral impurities are subjected to transport across the magnetic field due to their unimpeded motion during the short atomic phases.⁸ Poloidal asymmetry of the impurity density, which occurs because of the rotation, results in an enhancement of diffusivity.⁹ All these effects will add to a diffusion which will further widen what is presented in the present simulation as a "bump." The electric field is dominantly increasing in the region of the gradient and reaches its peak on the low density side of the profile at the bottom of the gradient. It is therefore our belief that a speculation on the possible role of such a positive electric field on the transport barrier is appropriate.

Finally, the results in Figs. 2(c), 2(d), 4(c), and 4(d) give the effects of the impurity concentration and of the ratio m_i/m_e on the solution. In particular, the solution is sensitive to the ratio m_i/m_e since it modifies the gyro-radius through the factor $(m_i/m_e)^{1/2}$. The factor m_i/m_e is usually higher in most tokamaks than the value of 10 taken in the present work. However, the finite dimension of our simulation box and the pertinence of the gyro-kinetic equations impose some restriction on increasing m_i/m_e in the present simulations. Having established the 1D nature of the solution, work is in progress to apply a fully kinetic 1D code (three velocity dimensions) to the present problem.

An ion's gyro-radius plays an important role in the formation of a charge separation at a plasma edge, in the presence of a steep gradient. The physics of this charge separation is important not only in tokamak physics. For instance, the existence of a shear layer at the edge of the reversed field experiment (RFX) has been recently reported,¹⁰ with a shearing rate level comparable to tokamaks in the high-confinement mode (H -mode). For the parameters of RFX, the ratio of $\rho_i/\lambda_{De} \approx 100$. Attempts to explain the existence of this shear layer by a model which calculates the effect of unconfined ion orbits on particle and momentum at the edge of the plasma in RFX has been recently reported.¹¹ We see in the present results that the combined effect of a gradient and large ratio of ρ_i/λ_{De} results in a charge separation and an electric field at a plasma edge due to the large orbits of the ions. The importance of impurity ions in the physics of the edge has long been pointed out.^{3,4} Even a small fraction of impurity ions can seriously modify the charge separation and the electric field at the edge, due to the fact that impurity ions, with their large gyro-radii, can add a charge contribution in the low density regions at the edge where the main ions, with a smaller gyro-radius, cannot provide a contribution. In addition, these ions with large gyro-radius can drift and diffuse across the magnetic field, and it has also been recently pointed out in Ref. 2 that a very small diffusion at a plasma edge can lead to important modifications of the charge and the electric field at the plasma edge. We also point to the recent experimental result in the Frascati tokamak (FTU) where the injection of a krypton impurity resulted in a sudden increased poloidal rotation.⁷ The impurity ion's profile plays an important role in the results we are presenting. We have used a profile for the impurity ions similar to the profile of the major ion species. However, im-

purity ions can be placed farther to the left of the ion profile in Fig. 1, which will increase their contribution to the charge and to the electric field at the edge. It has also been pointed out in Ref. 3 that the profile of the impurity ions can sometimes lead to instabilities. The physics of the transition at the edge of a plasma with the formation of an electric field seems to be a challenging subject. Work is underway to further studies on these problems, including a 1D fully kinetic code (1D in space and three velocity dimensions), and a gyro-kinetic code with three spatial dimensions.¹² Eulerian Vlasov codes, having a very low noise level, offer a powerful tool for this investigation. Finally, we note that the region of the divertor in a tokamak is a region rich with impurities. In view of the present results, one expects an important electric field to be present at the plasma edge in this region, and one can speculate that this electric field will certainly play a role in the divertor region, especially in what is called a detached plasma. This is under investigation.

The Center Canadien de fusion magnétique is funded by Hydro-Québec and by the Institut National de la Recherche Scientifique.

^aPresent address: Forschungszentrum Seibersdorf, Seibersdorf, Austria.
Electronic mail: shoucri@ccfm.ireq.ca

^bPresent address: LPMI URA 835, Université Henri Poincaré, Nancy, France.

^cPresent address: Department of Physics and Astronomy, University of Iowa, Iowa.

¹G. Manfredi, M. Shoucri, R. Dendy, A. Ghizzo, and P. Bertrand, *Phys. Plasmas* **3**, 202 (1996).

²M. Shoucri, G. Manfredi, P. Bertrand *et al.*, "Charge separation velocity shear and suppression of turbulence at a plasma edge in the gyrokinetic approximation," *J. Plasma Phys.*, accepted for publication; see also M. Shoucri, J. Lebas, G. Knorr, P. Bertrand, A. Ghizzo, G. Manfredi, and I. Christopher, *Phys. Scr.* **57**, 283 (1998).

³B. Coppi, H. P. Furth, M. N. Rosenbluth, and R. Z. Sagdeev, *Phys. Rev. Lett.* **17**, 377 (1966).

⁴B. Coppi, in *Proceedings of 13th International Conference Plasma Physics and Controlled Fusion*, Washington, D.C., 1990 (International Atomic Energy Agency, Vienna, 1991), Vol. 2, p. 413.

⁵See, for instance, the JET team, paper presented by C. Gormezano "High Performance with Modified Shear in JET D-D and D-T Plasmas," *Proceedings of 17th International Conference on Plasma Physics and Controlled Fusion*, Japan, 1998 (International Atomic Energy Agency, Vienna, to be published); R. Weynants "Overview of RI mode results on TEXTOR-94," *ibid.*

⁶G. Manfredi, M. Shoucri, P. Bertrand *et al.*, *Phys. Scr.* **58**, 159 (1998).

⁷D. Pacella, B. Gregory, M. Leigheb *et al.*, in *Proceedings of 25th EPS Conference on Controlled Fusion and Plasma Physics* Prague, 1998 (European Physical Society, Petit-Lancy, Switzerland, 1998).

⁸G. Fussman, *Contrib. Plasma Phys.* **37**, 363 (1997); P. Helander, S. Krasheninnikov, and P. J. Cato, *Phys. Plasmas* **1**, 3174 (1994).

⁹M. Romanelli and M. Ottaviani, *Plasma Phys. Controlled Fusion* **40**, 1767 (1998).

¹⁰V. Antoni, D. Desideri, E. Martines *et al.*, *Phys. Rev. Lett.* **79**, 4814 (1997).

¹¹R. Bartiromo, *Phys. Plasmas* **5**, 3342 (1998).

¹²M. Shoucri, G. Manfredi, P. Bertrand *et al.*, in *Proceedings of 25th EPS Conference on Controlled Fusion and Plasma Physics*, Prague, 1998 (European Physical Society, Petit-Lancy, Switzerland, 1998).